Communication

Probing the Structure of CH_2^+ by Dissociative Charge Exchange

Jennifer E. Mann, Zhen Xie, John D. Savee, Bastiaan J. Braams, Joel M. Bowman, and Robert E. Continetti

J. Am. Chem. Soc., **2008**, 130 (12), 3730-3731 • DOI: 10.1021/ja0782504

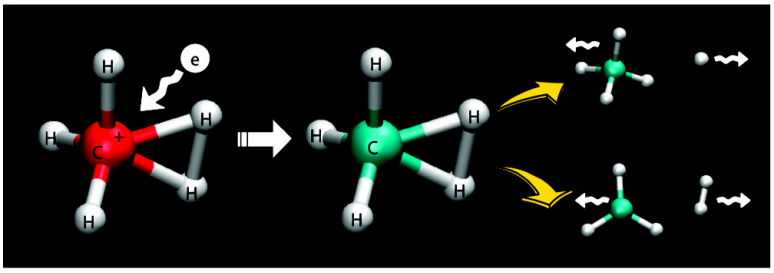

More About This Article

Additional resources and features associated with this article are available within the HTML version:

- Supporting Information
- Links to the 1 articles that cite this article, as of the time of this article download
- Access to high resolution figures
- Links to articles and content related to this article
- Copyright permission to reproduce figures and/or text from this article

View the Full Text HTML

J|A|C|S
COMMUNICATIONS

Published on Web 02/28/2008

Probing the Structure of CH_5^+ by Dissociative Charge Exchange

Jennifer E. Mann,† Zhen Xie,‡ John D. Savee,† Bastiaan J. Braams,‡ Joel M. Bowman,*,‡ and Robert E. Continetti*,†

Department of Chemistry and Biochemistry, University of California, San Diego, 9500 Gilman Drive, La Jolla, California 92093-0340, and Department of Chemistry and Cherry L. Emerson Center for Scientific Computation, Emory University, Atlanta, Georgia 30322

Received October 29, 2007; E-mail: rcontinetti@ucsd.edu; jmbowma@emory.edu

The simplest nonclassical carbonium ion is CH_5^+.[1] It is an important ion in the interstellar medium, where it is formed via radiative association of CH_3^+ and H_2.[2] The ion was first observed in a mass spectrum in the 1950s[3] and later shown to dissociate upon neutralization by charge exchange.[4] However, it has only been within the past 10 years that Oka and co-workers were able to measure its high resolution infrared spectrum.[5] The highly fluxional character of the CH_5^+ zero-point wave function and the "quantum deconstruction" of the IR spectrum using a global potential energy surface (PES) was recently reported.[6] The H atoms freely exchange by passage over low energy isomerization barriers of C_s and C_{2v} symmetry. The neutralization of CH_5^+ by dissociative recombination with free electrons is of importance in astrophysics, and there has been some controversy about the product branching ratios from ion storage ring and flowing afterglow measurements.[7,8] From a fundamental perspective the attachment process serves as a probe of the nascent phase space of CH_5^+.

In the current work, the product branching ratios in the dissociative charge exchange (DCE) of CH_5^+ with Cs are examined and compared to predictions using quasiclassical trajectory calculations on accurate *ab initio* potential energy surfaces. In these experiments, fragment channels (1) and (2) are detected in coincidence, yielding product kinetic energy release (KER) distributions and the branching ratios.

$$CH_5 \rightarrow CH_4 + H \quad (1)$$

$$CH_5 \rightarrow CH_3 + H_2 \quad (2)$$

The comparison with theory provides experimental evidence for the fluxional nature of CH_5^+.

The experimental apparatus has been described elsewhere and will only be discussed briefly.[9] CH_5^+ was formed with a pulsed discharge in a supersonic expansion (1 kHz) with a 1:9:60 CH_4/Ar/H_2 mixture. This source is expected to produce CH_5^+ with a rotational temperature of 20−60 K and a vibrational temperature less than 1660 K as discussed further in the Supporting Information (SI). The cations were skimmed, accelerated to 16 keV, and mass-selected by time-of-flight. Before reaching the Cs cell all ions with the exception of CH_5^+ are deflected. The transient CH_5 is formed when it is passed through an ~1 mm^3 interaction region containing ~1×10^{-5} Torr of Cs. Remaining CH_5^+ is deflected into an ion detector. The neutral fragments fly ~110 cm to a multiparticle time- and position-sensitive detector. Using this information along with the parent mass and ion beam velocity, the fragment masses and center-of-mass KER of each dissociation channel can be calculated, yielding experimental N(KER) distributions. These experimental distributions are corrected to yield P(KER) probability distributions by accounting for any loss of products owing to the kinematics as discussed in the Supporting Information (SI). Integration of the P(KER)s over KER yields product branching ratios from a single data set.

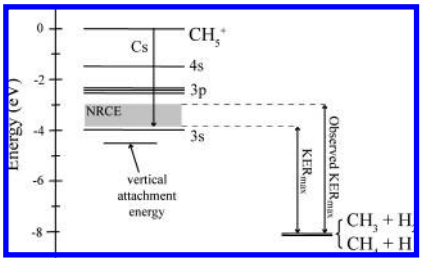

Figure 1. Energy level diagram showing the two energetically accessible dissociation limits of CH_5 and where on the neutral surface the CH_5 is formed via DCE with Cs. The three-body dissociation limit is nearly resonant with the 3s state and was not observed.

To simulate the experiment, quasiclassical trajectory (QCT) calculations were performed in the classical Franck−Condon approximation, i.e., by making vertical transitions from the CH_5^+ phase space to CH_5 using an *ab initio* PES for CH_5.[10] The CH_5^+ phase space was obtained from trajectories with the quantum zero-point energy of roughly 11000 cm^{-1} on an *ab initio* CH_5^+ PES.[11] In addition to these vertical trajectories, two other batches were run with initial kinetic energy to be consistent with the experiment for the "resonant" and "nonresonant" cases, as described below and in detail in the SI. Product branching ratios, internal energy distributions, and the KER distributions were obtained from roughly 25000 trajectories with zero total angular momentum for each of these cases. For diagnostic purposes, trajectories were also performed at the CH_5^+ equilibrium geometry with standard normal mode sampling of initial conditions appropriate for a semirigid molecule[12] for both the vertical transition and the nonresonant case.

Experimentally, the neutral CH_5 is formed slightly (~0.1 eV) above the predicted energy of the 3s Rydberg state,[13] rather than directly on the ground neutral surface, as assumed in the calculations. The transition to the neutral surface is assumed to be vertical. The two lowest dissociation channels are nearly isoenergetic as shown in Figure 1. Although H_2 loss is kinematically more favorable to detect, H atom loss is found to be the dominant dissociation channel.

The difference in energy between the ground vibrational state of $CH_5^+ + e^-$ and the dissociation limit of $CH_4 + H$ from the present PESs is 8.0 eV, in agreement with the experimental estimate of 8.0 ± 0.5 eV.[14] (This is further discussed in the SI.) For the case of resonant charge exchange with Cs, the neutral is formed 3.9 eV below the cation, yielding a maximum KER (KER_{max}) of 4.1 eV, approximately the same for both product channels.

† University of California.
‡ Emory University.

10.1021/ja0782504 CCC: $40.75

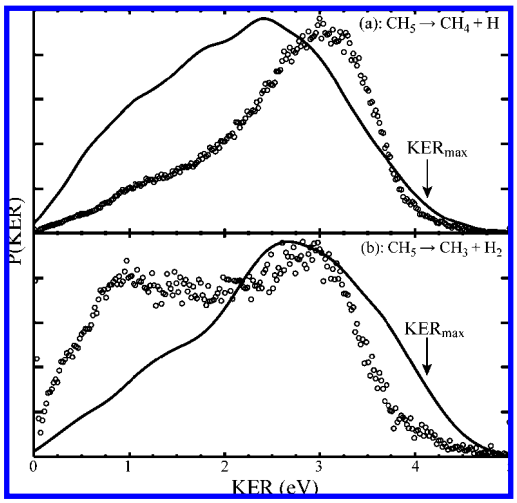

Figure 2. (a) P(KER) distribution for $CH_5 \rightarrow CH_4 + H$ and (b) $CH_5 \rightarrow CH_3 + H_2$. The open circles represent the experimental KER, while the solid line is the theoretical KER, with KER_{max} noted.

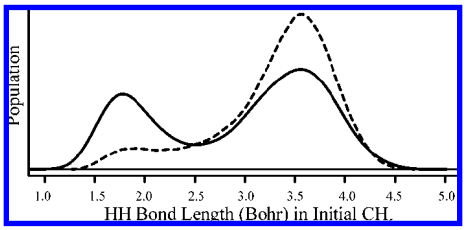

Figure 3. Classical HH bond length distribution of CH_5^+ with zero-point energy (dashed curve) and magnified part of that distribution that correlates with the $CH_3 + H_2$ products. The shoulder near 2.0 Bohr corresponds to the H_2 moiety, whereas the peak at 3.5 Bohr corresponds to the H−H distances with H atoms in the CH_3 group.

However, the experimentally observed KER_{max} is ~5 eV. This may be a result of some vibrational excitation in CH_5^+ as well as nonresonant charge exchange[15] leading to the production of neutral states above the resonant level. Experimentally, the branching ratio is 11 ± 2:1, for H loss to H_2 loss. The results from the three batches of trajectories described above using the correct "fluxional" phase-space sampling of CH_5^+ are 14:1 (vertical), 11:1 (resonant), and 9:1 (nonresonant) in very good accord with the experiment. The results from standard mode sampling are 34:1 (vertical) and 18:1 (nonresonant) which are not in agreement with experiment. This result provides a strong consistency argument for the fluxional nature of the parent CH_5^+ cation determining the experimental branching ratio.

The P(KER) for the dominant channel, $CH_4 + H$, is shown in Figure 2a, along with the theoretical prediction. Both exhibit a peak with a shoulder at lower energy. It is clear that most of the energy goes into internal excitation (vibrational and rotational) of the CH_4, as shown by the small probability for products at KER_{max}.

The P(KER) for the molecular hydrogen loss channel is shown in Figure 2b. This channel exhibits a bimodal distribution, with peaks at 1.0 and 2.9 eV. The theoretical KER peaks at approximately 2.8 eV but does not reveal the bimodal distribution seen experimentally; however, a shoulder at around 1.3 eV is observed.

The explanation for this shoulder comes from consideration of the HH bond length distribution in the parent CH_5^+ and more significantly the portion of that distribution that correlates with $CH_3 + H_2$ products; both are shown in Figure 3. The full classical distribution, which agrees well with quantum diffusion Monte Carlo calculations,[16] is bimodal with a short bond length corresponding to the H_2 moiety in CH_5^+ and a long bond length arising from the other HH distances. The distribution correlating with $CH_3 + H_2$ shows a larger contribution from the short HH distance than the long one. Examination of the trajectories leading to highly vibrationally excited H_2 indicates a greater contribution from the large HH bond length in the correlated distribution than from the short HH bond length. It is important to note that the corresponding correlated distribution from the normal mode sampling is unimodal for both the vertical and nonresonant cases with a peak at the HH-moiety equilibrium distance. Also the corresponding $CH_3 + H_2$ P(KER) for the nonresonant case shows less probability at low KER than that seen for the theoretical P(KER) with fluxional phase space sampling shown in Figure 3. The vibrational distributions of CH_3 and H_2 are shown in the SI.

QCT calculations are not exact dynamics, and there are also uncertainties in the CH_5 PES. However, both represent the current, feasible state-of-the-art calculations for a problem this complex. With these caveats in mind, the agreement between the experimental and theoretical branching ratios provides evidence that the quantum mechanically predicted fluxional nature of CH_5^+ [16] is responsible for the experimental branching ratio. However, the lack of quantitative agreement between the calculations and experiment for the more dynamically detailed KERs, in particular, the bimodal distribution in the $CH_3 + H_2$ channel, may indeed result from these caveats. Neglect of the coupling of the 3s Rydberg state to the ground electronic state in the present calculations may also play a role in the discrepancy.

DCE experiments on selected isotopologues of CH_5^+, namely $CD_3H_2^+$, CD_4H^+, and CD_5^+, have also been performed. Comparison of those results with QCT simulations will be reported and discussed in a later publication.

Acknowledgment. J.E.M., J.D.S., and R.E.C. thank the AFOSR (Grant FA9550-04-1-0035). Z.X. thanks the NSF (Grant CHE-0446527), and B.J.B. and J.M.B. thank the ONR (Grant N00014-05-0460).

Supporting Information Available: Branching ratio calculations; detection efficiency; ion temperature; details of QCT calculations and energetics. This material is available free of charge via the Internet at http://pubs.acs.org.

References

(1) Olah, G. A.; Klopman, G.; Schlosberg, R. H. *J. Am. Chem. Soc.* **1969**, *91*, 3261.
(2) Herbst, E.; Bates, D. R. *Astrophys. J.* **1988**, *329*, 410.
(3) Tal'roze, V. L.; Lyubimova, A. K. *Dokl. Akad. Nauk SSSR* **1952**, *86*, 909.
(4) Bordas-Nagy, J.; Holmes, J. L.; Hop, C. E. C. A. *Int. J. Mass Spectrom. Ion Proc.* **1988**, *85*, 241.
(5) White, E. T.; Tang, J.; Oka, T. *Science* **1999**, *284*, 135.
(6) Huang, X. C.; McCoy, A. B.; Bowman, J. M.; Johnson, L. M.; Savage, C.; Dong, F.; Nesbitt, D. J. *Science* **2006**, *311*, 60.
(7) Adams, N. G.; Herd, C. R.; Geoghegan, M.; Smith, D.; Canosa, A.; Gomet, J. C.; Rowe, B. R.; Queffelec, J. L.; Morlais, M. *J. Chem. Phys.* **1991**, *94*, 4852.
(8) Semaniak, J.; Larson, A.; Le Padellec, A.; Stromholm, C.; Larsson, M.; Rosen, S.; Peverall, R.; Danared, H.; Djuric, N.; Dunn, G. H.; Datz, S. *Astrophys. J.* **1998**, *498*, 886.
(9) Hanold, K. A.; Luong, A. K.; Clements, T. G.; Continetti, R. E. *Rev. Sci. Instrum.* **1999**, *70*, 2268.
(10) Xie, Z.; Bowman, J. M.; Zhang, X. B. *J. Chem. Phys.* **2006**, *125*, 133120.
(11) Jin, Z.; Braams, B. J.; Bowman, J. M. *J. Phys. Chem. A* **2006**, *110*, 1569.
(12) Hase, W. H. *Encyclopedia of Computational Chemistry*; Schleyer, P. v. R., Ed.; John Wiley & Sons, Ltd.: Cambridge, 1998; pp 399ff.
(13) Raynor, S.; Herschbach, D. R. *J. Phys. Chem.* **1982**, *86*, 3592.
(14) Griffiths, W. J.; Harris, F. M.; Brenton, A. G.; Beynon, J. H. *Int. J. Mass Spectrom. Ion Proc.* **1986**, *74*, 317.
(15) Laperle, C. M.; Mann, J. E.; Clements, T. G.; Continetti, R. E. *Phys. Rev. Lett.* **2004**, *93*, 153202.
(16) McCoy, A. B.; Braams, B. J.; Brown, A.; Huang, X. C.; Jin, Z.; Bowman, J. M. *J. Phys. Chem. A* **2004**, *108*, 4991.

JA0782504